Unsymmetrical Low-Generation Cationic Phosphorus Dendrimers as a Nonviral Vector to Deliver MicroRNA for Breast Cancer Therapy

Yu Zou, Siyan Shen, Andrii Karpus, Huxiao Sun, Regis Laurent, Anne-Marie Caminade, Mingwu Shen, Serge Mignani, Xiangyang Shi, Jean-Pierre Majoral

Unsymmetrical Low-Generation Cationic Phosphorus Dendrimers as a Nonviral Vector to Deliver MicroRNA for Breast Cancer Therapy

Yu Zou[1,2#], Siyan Shen[3#], Andrii Karpus [1,2], Huxiao Sun[3], Regis Laurent[1,2], Anne-Marie Caminade[1,2], Mingwu Shen[3], Serge Mignani[4], Xiangyang Shi[3,4]*, Jean-Pierre Majoral[1,2]*

[1] Laboratoire de Chimie de Coordination du CNRS, 205 route de Narbonne, 31077, Toulouse Cedex 4, France

[2] Université Toulouse 118 route de Narbonne, 31077, Toulouse Cedex 4, France

[3] State Key Laboratory for Modification of Chemical Fibers and Polymer Materials, Shanghai Engineering Research Center of Nano-Biomaterials and Regenerative Medicine, College of Biological Science and Medical Engineering, Donghua University, Shanghai 201620, China

[4] CQM-Centro de Química da Madeira, MMRG, Universidade da Madeira, Campus Universitário da Penteada, 9020-105 Funchal, Portugal

---

# These authors contributed equally to this work.

* To whom correspondence should be addressed. E-mail: jean-pierre.majoral@lcc-toulouse.fr (J. P. Majoral) and xshi@dhu.edu.cn (X. Shi)

Abstract

Development of nonviral dendritic polymers with simple molecular backbone and great gene delivery efficiency to effectively tackle cancer still remains a great challenge. Phosphorous dendrimers or dendrons are promising vectors due to their structural uniformity, rigid molecular backbone and tunable surface functionalities. Here, we report the development of a new low-generation unsymmetrical cationic phosphorus dendrimers bearing 5 pyrrolidine groups and one amine group as a nonviral gene delivery vector for cancer therapy. We show that hexachlorocyclotriphosphazene can be used as a core to finely create AB_5 type dendrimers and be protonated to form unsymmetrical cationic dendrimers with great water solubility and stability. The cationic unsymmetrical dendrimers with simple molecular backbone can compress microRNA-30d (miR-30d) to form polyplexes with desired hydrodynamic sizes and surface potentials, and can effectively transfect miR-30d to cancer cells at an optimal N/P ratio of 10. The dendrimer/miR-30d polyplexes display good cytocompatibility, and can transfect miR-30d to suppress the glycolysis-associated SLC2A1 and HK1 expression, thus significantly inhibiting the migration and invasion of a murine breast cancer cell line *in vitro* and the corresponding subcutaneous tumor mouse model *in vivo*. The developed unsymmetrical low-generation phosphorus dendrimers with simple molecular backbone and great gene delivery efficiency may be extended to deliver other genetic materials to tackle other diseases.

Keywords: unsymmetrical phosphorous dendrimers; microRNA delivery; tumor therapy

1. Introduction

Gene therapy has been widely used to treat different diseases (e.g., cancer and infectious diseases) by transfecting exogenous genetic materials such as plasmid DNA, messenger RNA or short-interfering RNA to target cells to result in the associated protein expression or gene silencing.[1-3] Among the widely used genetic materials, microRNA (miR) has aroused extensive interest.[4-7] As a kind of non-coding RNA, miRs are single-stranded endogenous small RNA with a length of approximately 20-24 nucleotides, and can negatively regulate gene expression post-transcriptionally by inhibiting translation and degrading target messenger RNA.[8-9] In cancer biology, miR deregulation is known to be involved in the occurrence of many types of cancer, and miR has been found to play an essential role in cell proliferation,[4, 10-11] differentiation,[12-14] angiogenesis[15-17] and apoptosis.[18] Hence, regulation of miR has been recognized as a compelling new therapeutic method to tackle cancer.

MicroRNA-30d (miR-30d) has been reported in the past few years for its excellent performance in the treatment of various cancer types, such as pancreatic ductal adenocarcinoma[19] and breast cancer.[20] MiR-30d is closely associated to the metabolism and proliferation of cancer cells, and overexpression of miR-30d can effectively prevent the proliferation and colony formation of cancer cells. In general, miR-30d is considered to be a glycolysis-associated miR that inhibits glycolysis in cancer cells.[19]

Due to the negative surface charge, naked miRs have difficulty to cross the cell membrane to complete the gene transfection process. Since viral vectors have generated serious safety concerns,[21] nonviral vectors such as cationic polymers, liposomes, and dendrimers have been widely applied to deliver genetic materials to target cells.[22-23] The major advantages of nonviral vectors are as follows: low immunogenicity and oncology impact, high gene loading capacity, and tunable surface modification.[9] Applicable nonviral vectors should be easily synthesized, simple and precise molecular backbones, good stability, easy surface modification, and biocompatibility.

Phosphorus dendrimers or dendrons, due to their good biocompatibility and the presence of a

large number of modifiable sites on the surface and branches, have been shown to have excellent performance in drug delivery,[24-25] gene transfection[16, 26-28] and drug active *per se*.[29-32] Their relatively convenient synthesis method also allows the development of various nanoparticulate systems to tackle a wide range of diseases. Our earlier work has shown that phosphorus dendrimers bearing pyrrolidinium or piperidinium on their surface can be used for gene delivery to treat breast cancer.[26] As controversy to poly(amidoamine) (PAMAM) dendrimers, for cationic phosphorous dendrimers, a lower generation dendrimers bearing the same cyclic amines display much higher gene delivery efficiency than the higher generation counterparts. This could be due to the highly rigid dendritic structure of phosphorus dendrimers, which is opposed to PAMAM dendrimers. Furthermore, we have also shown that core-shell tecto dendrimers with phosphorus dendrimers as a core display much higher gene delivery efficiency[33] and amplified enhanced permeability and retention effect for improved tumor penetration and retention,[34] which are desired for cancer therapy applications. All these merits are attributable to the highly rigid structure of phosphrous dendrimers, which stimulates our further efforts to develop nonviral dendritic polymers with simple molecular backbone for improved gene delivery to effectively tackle cancer.

In comparison to symmetric low-generation phosphorus dendrimers, unsymmetric structure of phosphorus dendrimers with modifiable functional termini provides more opportunities to design phosphorous dendrimer-based nanomedicines or functional delivery systems for various biomedical applications. The unsymmetrical low-generation cationic phosphorus dendrimers should not display compromised gene delivery efficiency. On this basis, in this work, we attempted to design a type of unsymmetrical low-generation cationic phosphorus dendrimers as a vector to deliver miR-30d for gene therapy of breast cancer. The unsymmetric phosphorus dendrimers bearing 5 pyrrolidine groups and one primary amine group were synthesized with the common hydrazine phosphonate group incorporated within the branch (Figure 1). After protonation, the cationic phosphorus dendrimers were formed and complexed with miR-30d to generate dendrimer/miR-30d polyplexes. The synthesized dendrimers and dendrimer/miR-30d polyplexes were thoroughly characterized through different

techniques. The polyplexes were examined in terms of their cytotoxicity, cellular transfection efficiency, and protein expression *in vitro* and the miR-30d delivery-mediated cancer therapeutic efficacy was examined by treating a subcutaneous murine breast cancer model. To our knowledge, this is the very first example to develop an unsymmetrical cationic phosphorus dendrimer-based nonviral vector with simple molecular backbone to delivery miR for cancer therapy applications.

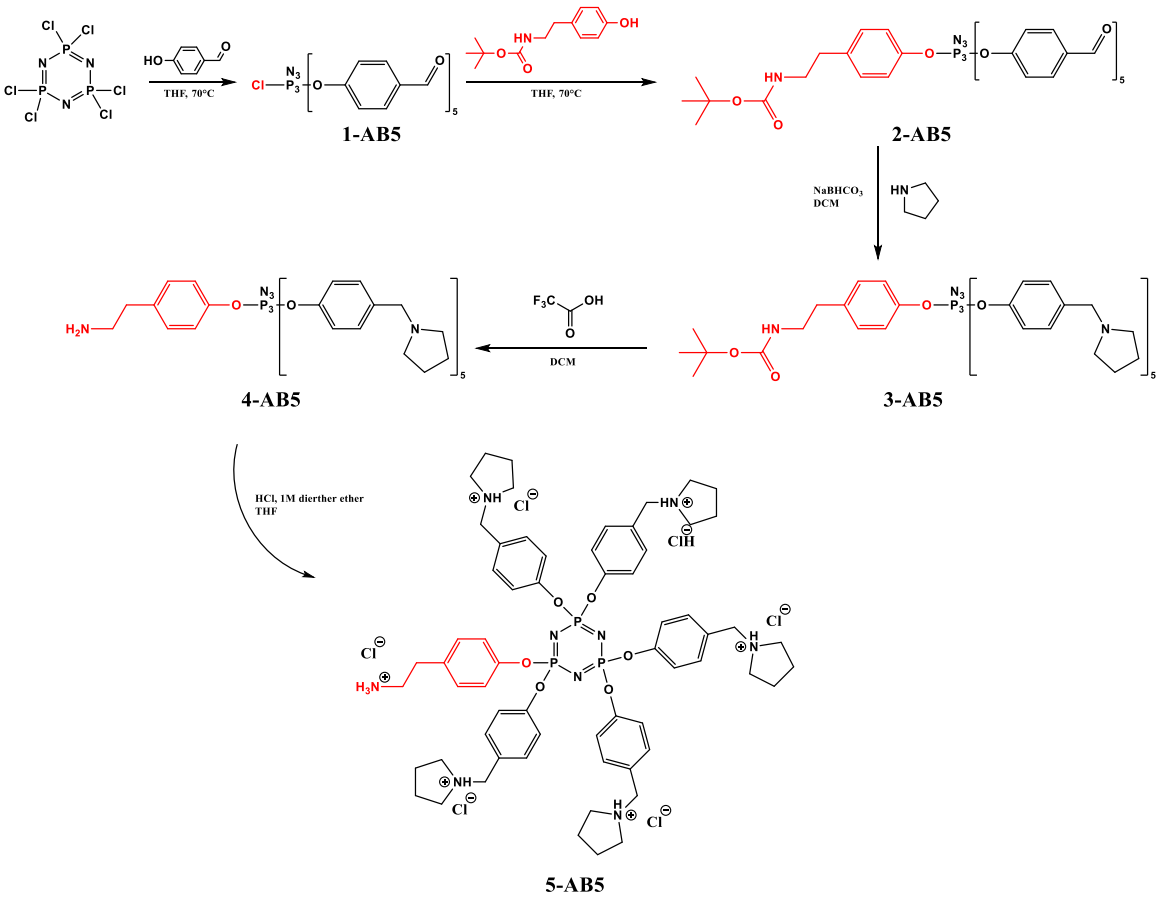

Figure 1. Synthesis of unsymmetrical cationic phosphorus dendrimer.

2. Experiment Section

Synthesis of Unsymmetrical Phosphorus Dendrimer (1-AB$_5$). The solution of hexachlorocyclotriphosphazene (4.52 mmol, 1.57 g, in 30 mL tetrahydrofuran (THF)) was added into the mixture of 4-hydroxybenzaldehyde (22.60 mmol, 2.75 g) and potassium carbonate (45.20 mmol, 14.72 g) in 50 mL THF at 0 °C. The reaction mixture was stirred overnight at room temperature. Salts were then removed by centrifugation and the supernatant was concentrated under reduced pressure.

The residue was then purified by silica column chromatography (hexane/ethyl acetate, 8/2 to 6/4, v/v) to afford 1-AB5 dendrimer as a colorless oil in a 76% yield. **^{1}H NMR (400 MHz, CDCl3)** δ = 10.0 – 9.9 (m, 5H, $C_5\underline{H}O$), 7.9 – 7.8 (m, 2H, $C_2\underline{H}$-C_3H), 7.3 – 7.2 (m, 2H, C_2H-$C_3\underline{H}$) ppm. **^{31}P NMR** (162 MHz, CDCl3) δ = 20.7 (t, J=86.3, $\underline{P}_3$), 5.2 (d, J=86.1, $\underline{P}_1$, $\underline{P}_2$) ppm. **^{13}C{^{1}H} NMR (100 MHz, CDCl3)** δ= 121.40 (m, C_2), 131.44 (s, C_3), 133.77 (m, C_4), 154.29 (m, C_1), 190.36 (s, C_5), 190.48 (s, C_5) ppm.

Synthesis of N-Boc-tyramine-Modified Unsymmetrical Phosphorus Dendrimer (2-AB$_5$). N-Boc-tyramine (0.673 g, 2.835 mmol) and potassium carbonate (0.748 g, 2.835 mmol) were added to a solution of 1-AB$_5$ (2 g, 2.577mmol, in 100 ml acetonitrile) while stirring overnight at 92 °C. The reaction mixture was extracted with 1M NaOH aqueous solution, dichloromethane (DCM), water and brine. After that, the organic phase was concentrated with a rotary evaporator to obtain 2-AB$_5$ as a white powder (yield = 97.3%). **^{1}H NMR (400 MHz, CDCl3)** δ = 9.9 (d, J=4.2, 5H, $C_{14}\underline{H}O$), 7.7 (dd, J=3.2, 8.7, 10H, $C_{11}H$-$C_{12}\underline{H}$), 7.1 (dd, J=8.3, 20.4, 10H, $C_{11}\underline{H}$-$C_{12}H$), 7.0 (d, J=8.3, 2H, $C_7\underline{H}$-C_8H), 6.9 (d, J=8.4, 2H, C_7H-$C_8\underline{H}$), 4.6 (t, J=5.6, 5.6, 1H, NH), 3.3 (q, J=6.9, 6.9, 6.9, 2H, NH-$C_4\underline{H}_2$), 2.8 (t, J=7.3, 7.3, 2H, C_4H_2-$C_5\underline{H}_2$), 1.4 (s, 9H, $C_1\underline{H}_3$) ppm. **^{31}P {^{1}H} NMR** (162 MHz, CDCl3) δ = 7.6 – 7.3 (m, P=N) ppm. **^{13}C {^{1}H} NMR (101 MHz, CDCl3)** δ= 190.7 – 190.4 (m, C_{14}), 154.8 (s, C_3), 154.6 (s, C_{10}), 148.5 (s, C_9), 136.7 (s, C_{13}), 133.8(s, C_6), 131.4 (s, C_{12}), 129.9(s, C_7), 121.3 (s, C_{11}), 120.7 (s, C_8), 79.3(s, C_2), 41.7(s, C_4), 35.5 (s, C_5), 28.4 (s, C_1) ppm.

Synthesis of Pyrrolidine-Modified Unsymmetrical Phosphorus Dendrimer (3-AB$_5$). 2-AB$_5$ (1.1 g, 1.126 mmol) and pyrrolidine (0.817 g, 11.49 mmol) were co-dissolved in 100 mL DCM, and the mixture was cooled down under an ice bath. And then, sodium triacetoxyborohydride (1.651 g, 13.522 mmol) was add to the above mixture solution while stirring vigorously overnight. The reaction mixture was purified with column chromatography (methanol: tryethylamine = 99: 1), and the 3-AB5 was obtained as a light-yellow powder (yield = 37%) after concentrated with a rotary evaporator. **^{1}H NMR (400 MHz, CDCl3)** δ = 7.2 – 7.1 (m, 10H, $C_{11}H$-$C_{12}\underline{H}$), 7.0 – 6.9 (m, 2H, $C_7\underline{H}$-C_8H), 6.9 – 6.9 (m, 12H, $C_{11}\underline{H}$-$C_{12}H$, C_7H-$C_8\underline{H}$), 3.6 (d, J=326.0, 10H, $C_{14}\underline{H}_2$-N), 3.3 (q, J=6.9, 6.9, 6.9, 2H, NH-$C_4\underline{H}_2$), 2.8 (t, J=7.2, 7.2, 2H, C_4H_2-$C_5\underline{H}_2$), 2.5 – 2.4 (m, 20H, N-$C_{15}\underline{H}_2$-$C_{16}H_2$), 1.8 – 1.7 (m, 20H,

$C_{15}H_2$-$C_{16}\underline{H_2}$), 1.4 (s, 9H, $C_1\underline{H_3}$) ppm. **^{31}P {^{1}H} NMR** (162 MHz, CDCl3) δ = 8.7 (t, J = 5.9 Hz, P=N) ppm. **^{13}C {^{1}H} NMR (101 MHz, CDCl3)** δ = 155.9 (s, C_3), 149.6 (s, C_{10}), 149.2 (s, C_9), 135.9 (s, C_{13}), 135.5 (s, C_6), 129.7 (s, C_{12}), 129.6 (s, C_7), 121.0 (s, C_{11}), 120.7 (s, C_8), 79.2(s, C_2), 60.0 (s, C_{14}), 54.1 (s, C_{15}), 41.6 (s, C_4), 35.3 (s, C_5), 28.4 (s, C_1), 23.4 (s, C_{16}).

Synthesis of Deprotected Unsymmetrical Phosphorus Dendrimer (4-AB5). The 3-AB5 (0.5 g, 0.398 mmol) was dissolved in 20 mL DCM, and excess trifluoroacetic acid was added dropwise to the above solution. The reaction were carried out under Ar while stirring overnight. The solution was extracted with 1 M NaOH aqueous solution and DCM each for 3 times. After extraction, organic phase was collected. The compound 4-AB5 was obtained as a deep red powder (yield = 94%) after evaporation and vacuum drying. **^{1}H NMR (400 MHz, CDCl3)** δ =7.1 (dd, J=3.4, 7.9, 10H, C_8H-$C_9\underline{H}$), 7.0 (d, J=8.5, 2H, $C_4\underline{H}$-C_5H), 6.9 (t, J=7.0, 7.0, 12H, $C_8\underline{H}$-C_9H, C_4H-$C_5\underline{H}$), 3.6 (s, 10H, $C_{11}\underline{H_2}$-N), 2.9 (t, J=6.9, 6.9, 2H, NH_2-$C_1\underline{H_2}$), 2.7 (t, J=6.9, 6.9, 2H, C_1H_2-$C_2\underline{H_2}$), 2.5 (t, J=5.2, 5.2, 20H, N-$C_{12}\underline{H_2}$-$C_{13}H_2$), 1.8 (t, J=5.2, 5.2, 20H, $C_{12}H_2$-$C_{13}\underline{H_2}$) ppm. **^{31}P {^{1}H} NMR** (162 MHz, CDCl3) δ = 8.7 (t, J=11.7, 11.7, P=N) ppm. **^{13}C {^{1}H} NMR (101 MHz, CDCl3)** δ = 149.6 (s, C_7), 149.1 (s, C_6), 136.3 (s, C_{10}), 135.8 (s, C_3), 129.7 (s, C_9), 129.6 (s, C_4), 121.0 (s, C_8), 120.7 (s, C_5), 59.9 (s, C_{11}), 54.1 (s, C_{12}), 43.6 (s, C_1), 39.4 (s, C_2), 23.5(s, C_{13}).

Synthesis of Cationic Unsymmetrical Phosphorus Dendrimer (5-AB5). The 4-AB5 (0.4 g, 0.346 mmol) was dissolved in THF (20 mL). Hydrochloric acid (excess) was added dropwise to the solution and the reaction was carried out at 40 °C under vigorous stirring. After vacuum drying, cationic unsymmetrical phosphorus dendrimers (5-AB5) were obtained as a deep red powder in around 97% yield. ^{1}H NMR (400 MHz, D2O) δ = 7.4 – 7.4 (m, 10H, C_8H-$C_9\underline{H}$), 7.2 (d, J=8.1, 2H, $C_4\underline{H}$-C_5H), 7.1 – 6.9 (m, 10H, $C_8\underline{H}$-C_9H), 6.9 (d, J=8.2, 2H, C_4H-$C_5\underline{H}$), 4.3 (s, 10H), 3.4 (s, 10H, $C_{11}\underline{H_2}$-N), 3.2 (t, J=7.6, 7.6, 2H, NH_3-$C_1\underline{H_2}$), 3.1 (s, 10H, $C_{11}\underline{H_2}$-N), 2.9 (t, J=7.6, 7.6, 2H, C_1H_2-$C_2\underline{H_2}$), 1.9 (d, J=73.8, 20H, $C_{12}H_2$-$C_{13}\underline{H_2}$) ppm. **^{31}P {^{1}H} NMR** (162 MHz, CDCl3) δ = 8.8 (s, P=N) ppm

Synthesis of Dendrimer/MiR-30d Polyplexes. The AB5 dendrimers were dissolved in water and mixed with miR-30d under different N/P ratios for 15 min at room temperature to prepare the 5-

AB5/miR-30d polyplexes. See additional experimental details in the Supporting Information.

3. Results and Discussion

Synthesis and Characterization of Unsymmetrical Phosphorus Dendrimers (5-AB5). All the unsymmetrical phosphorus dendrimer intermediates and final 5-AB5 dendrimers were fully characterized by NMR and/or mass spectrometry techniques (see details above, and Figure S1-15). Afterwards, we examined the hydrodynamic diameter and zeta potential of 5-AB5 dendrimers (Table S1). The hydrodynamic diameter of 5-AB5 dendrimers is 238 nm with a polydispersity index (PDI) of 0.52, while they have a positively charged surface potential (53.6 mV), which is favorable for gene delivery.

Synthesis and Characterization of Dendrimer/miR-30d Polyplexes. Firstly, in order to apply the 5-AB5 dendrimers for gene delivery, we used a PANOPA assay kit to determine the number of primary amines per dendrimer. Each 5-AB5 dendrimer was determined to have 24.9 primary amines on its surface, thus allowing for effective compression of negatively charged miR-30d through electrostatic interaction. According to different N/P ratios that are defined as the molar ratio of nitrogen in the surface group of cationic phosphorus dendrimers to miR-30d backbone phosphates, the 5-AB5 dendrimers were complexed with miR-30d to form the vector/miR-30d polyplexes. Then, agarose gel retardation assay was adopted to test the miR-30d compaction ability of the vector. As shown in Figure 2a, the miR-30d can be effectively compacted by 5-AB5, and the migration of miR-30d can be entirely blocked by 5-AB5 at an N/P ratio 1: 1 or above. These results indicate that the 5-AB5 dendrimers have a superior gene compression capability.

The dendrimer/miR-30d polyplexes formed at different N/P ratios were next characterized by dynamic light scattering and zeta potential measurements. As shown in Figure 2b, the 5-AB_5/miR-30d polyplexes display a hydrodynamic size of 238.0 ± 45.2 nm under different N/P ratios. In addition, zeta potential measurements reveal that all the 5-AB5/miR-30d complexes are positively charged with a surface potential in a range of 21.7 – 34.9 mV (Figure 2c). The zeta potential of 5-AB_5 dendrimers

decreases after electrostatic compaction of miR-30d, which could effectively improve their cytocompatibility and biosafety.

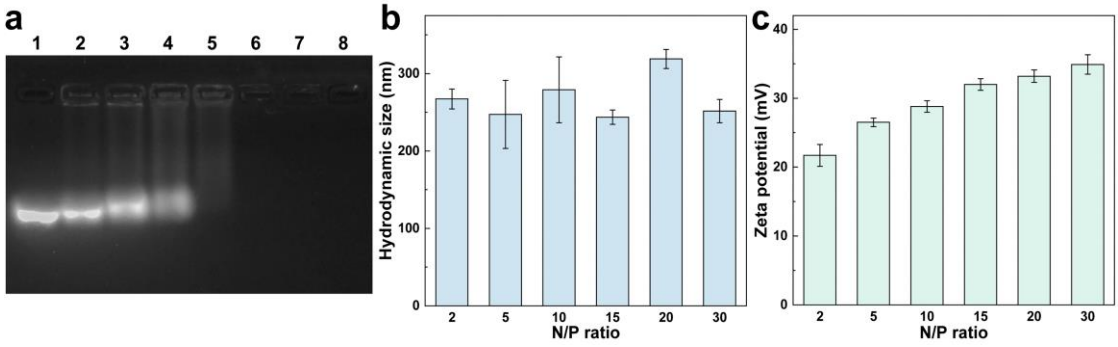

Figure 2. (a) Agarose gel retardation assay of miR-30d complexed with 5-AB_5 dendrimers under different N/P ratios (lane 1, free miR-30d, and lane 2-8, 5-AB_5/miR-30d polyplexes at an N/P values of 0.125, 0.25, 0.5, 1, 2, 3 and 4, respectively). (b) Hydrodynamic size and (c) zeta potential of the 5-AB5/miR-30d polyplexes at different N/P ratios.

In Vitro Cytotoxicity and Cellular Uptake Assays. The cytocompatibility of the gene vector is an important prerequisite for gene delivery. We then investigated the cytotoxicity of the 5-AB_5 and the 5-AB_5/miR-30d polyplexes by CCK-8 viability assay of 4T1 cells (a murine breast cancer cell line) before gene transfection studies. As shown in Figure 3a, with the increase of the 5-AB_5 concentration, the cell viability decreases, and reaches 57.4% at the concentration of 200 μM. At a given dendrimer concentration, cells treated with the 5-AB_5/miR-30d polyplexes display a higher viability than those treated with the 5-AB_5 alone, presumably because the surface positive charge of the vector is partially neutralized by the negatively charged miR-30d.

We then proceeded to investigate the cellular uptake behavior of the 5-AB5/miR-30d polyplexes, where the miR-30d was pre-labeled with FAM. After co-incubation of the 5-AB5/miR-30d-FAM polyplexes at different N/P ratios with 4T1 cells for 4 h, the cells were assayed flow cytometry and observed by confocal microscopy. As shown in Figure 3b-c, cells treated with PBS and free miR-30d do not show any obvious fluorescence signals. In contrast, cells treated with the 5-AB5/miR-30d polyplexes display apparent fluorescence signals, and the fluorescence intensity increases with the

increase of N/P ratio. At the N/P ratio of 10, cells display the peak fluorescence intensity and the fluorescence intensity starts to decrease at the N/P ratio of 15. This may be due to the increased cytotoxicity of the polyplexes at a relatively high N/P ratio, thus reducing the efficiency of gene transfection.

Afterwards, the optimal phagocytosis time of the 5-AB5/miR-30d polyplexes was investigated using confocal microscopy at an optimal N/P ratio of 10 (Figure 3d). As we can see, there is no obvious green fluorescence signal in 4T1 cells treated with PBS or free miR-30d. In sharp contrast, cells treated with the 5-AB5/miR-30d polyplexes display increased intracellular fluorescence intensity with the incubation time, and at 4 h incubation, the fluorescence intensity of cells appears to be saturated. Further extension of the incubation time to 6 h does not lead to any significant change in the fluorescence intensity of cells. Therefore, we selected the optimal phagocytosis time of 4 h for the subsequent experiments.

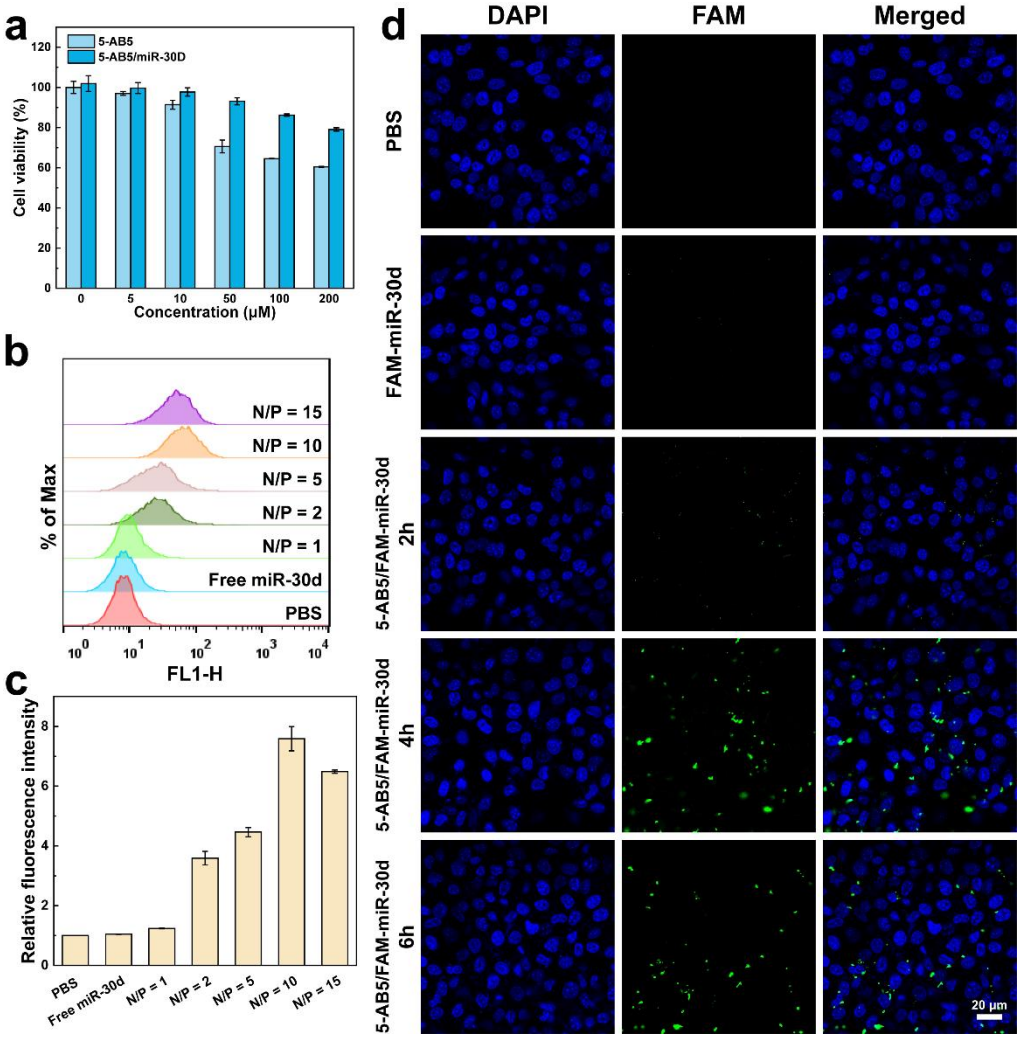

Figure 3. (a) CCK-8 viability assay of 4T1 cells treated with the dendrimers or polyplexes at different dendrimer concentrations for 24 h. Representative flow cytometry plots (b-c) and relative mean fluorescence intensity of 4T1 cells treated with PBS, free miR-30d, and 5-AB5/miR-30d under N/P values of 1, 2, 5, 10 and 15, respectively for 4 h. (d) Confocal microscopic images of 4T1 cells treated with PBS, free FAM-miR-30d or 5-AB5 complexed with FAM-miR-30d at an N/P ratio of 10 for 4 h. Cells treated with 5-AB5/FAM-miR-30d polyplexes for 2 and 6 h, respectively are also shown. Cell nucleus was stained with DAPI. Scale bar represents 20 μm for each panel.

In Vitro Inhibition of Cancer Cell Migration and Glycolysis. It has been reported that overexpression of miR-30d helps to inhibit cell migration and invasion, and studies have shown that the expression of miR-30d can inhibit the downstream proteins of SLC2A1 and HK1 by direct targeting of RUNX1, thus inhibiting cellular glycolysis to achieve antitumor effects.[19] The inhibitory property of cancer cell migration after miR-30d transfection by the 5-AB5/miR-30d polyplexes was assessed by cell scratch healing assay (Figure 4a-b). Clearly, 4T1 cells possess a high motility potential for metastasis with the migration area reaching 37.4% and 63.0% after incubation for 12 h and 24 h, respectively in the PBS group. However, this migration can be effectively inhibited with the treatment of free miR-30d and 5-AB5/miR-30d polyplexes. Among all groups, the group of 5-AB5/miR-30d polyplexes shows the strongest inhibition of 4T1 cell migration with 33.2% and 51.5% reduction in cell migration area at 12 h and 24 h, respectively when compared to the PBS group ($p < 0.001$). This suggests that 5-AB5/miR-30d can further amplify the ability of miR-30d to inhibit the migration of 4T1 cells by improving the delivery efficiency of gene which in turn can effectively inhibit tumor metastasis.

To confirm the inhibitory effect of miR-30d on SLC2A1 and HK1 in 4T1 cells *in vitro*, Western blot (WB) analysis was performed after the cells were transfected with the polyplexes (Figure 4c). Evidently, compared with groups of PBS, 5-AB5, and miR-30d, the 5-AB5/miR-30d group has the best inhibitory effect on the expression of SLC2A1 and HK1 proteins ($p < 0.001$). Overall, the

transfection of 5-AB5/miR-30d polyplexes can be expected to exert excellent anti-tumor effects by inhibiting the SLC2A1 and HK1 expression in 4T1 cells.

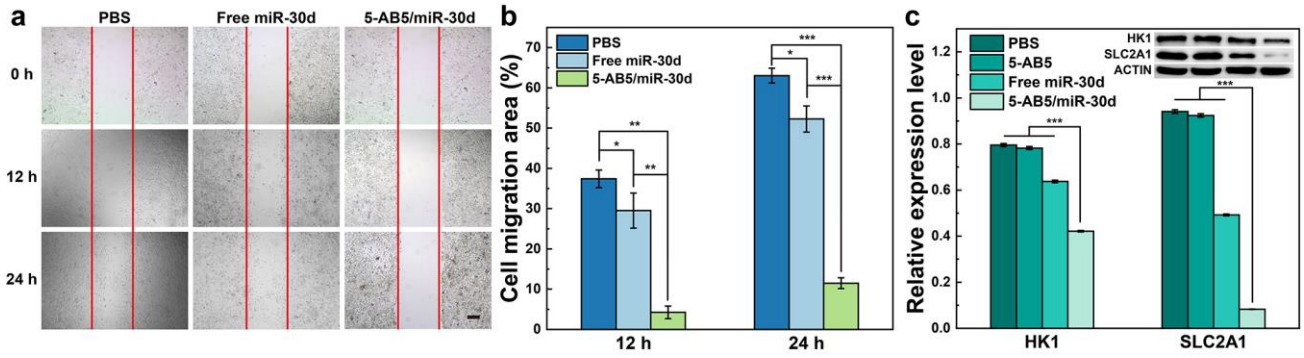

Figure 4. Cell scratch micrographs (a) and cell migration area (b) of 4T1 cells treated with PBS, free miR-30d, or 5-AB5/miR-30d polyplexes at different time points (scale bar = 200 μm for each panel, n = 3 for quantitative measurements of migration area). (c) Quantitative analysis of HK1 and SLC2A1 protein expressions from the WB assay data (inset). For b and c, * for $p < 0.05$, ** for $p < 0.01$, and *** for $p < 0.001$, respectively.

***In Vivo* 5-AB5/miR-30d Polyplex-Mediated Tumor Therapy.** Before utilizing 5-AB5/miR-30d for *in vivo* tumor therapy, hemolysis assay was carried out to evaluate their hemocompatibility (Figure S16). After incubation of mouse red blood cells (RBCs) with the 5-AB5/miR-30d at different concentrations, the hemolysis rates of mouse RBCs are all less than the threshold value of 5%,[35-36] indicating the excellent hemocompatibility of the polyplexes.

Inspired by the *in vitro* 5-AB5/miR-30d polyplex-mediated anticancer treatment, a xenografted 4T1 tumor model was next established to assess the therapeutic efficacy of 5-AB5/miR-30d polyplexes *in vivo*. Based on the treatment schedule, the 4T1 tumor-bearing mice were assigned to four groups (PBS, 5-AB5, free miR-30d and 5-AB5/miR-30d, respectively) and are treated *via* intratumoral injection (Figure 5a). Within the treatment period, the body weights of the tumor-bearing mice do not seem to have any significant changes after different treatments when compared to the PBS control group (Figure 5b), verifying the quite good biosafety profiles of all treatment materials. As shown in Figure 5c, the tumor volumes of the groups of PBS control, 5-AB5 and free miR-30d rapidly increase

over time. Strikingly, the tumors treated with the 5-AB5/miR-30d polyplexes display the most significant growth inhibition among all groups ($p < 0.001$). These results indicate that the developed 5-AB5 dendrimers have a promising miR-30d delivery efficiency *in vivo*. Further survival rate analysis shows that 60% of the tumor-bearing mice treated with the 5-AB5/miR-30d are still alive after 30 days, while at the same time point, the mice in the PBS, 5-AB5 and miR-30d groups are all dead (Figure 5d). Overall, the designed 5-AB5/miR-30d polyplexes enable the effective gene therapy of tumors *in vivo*.

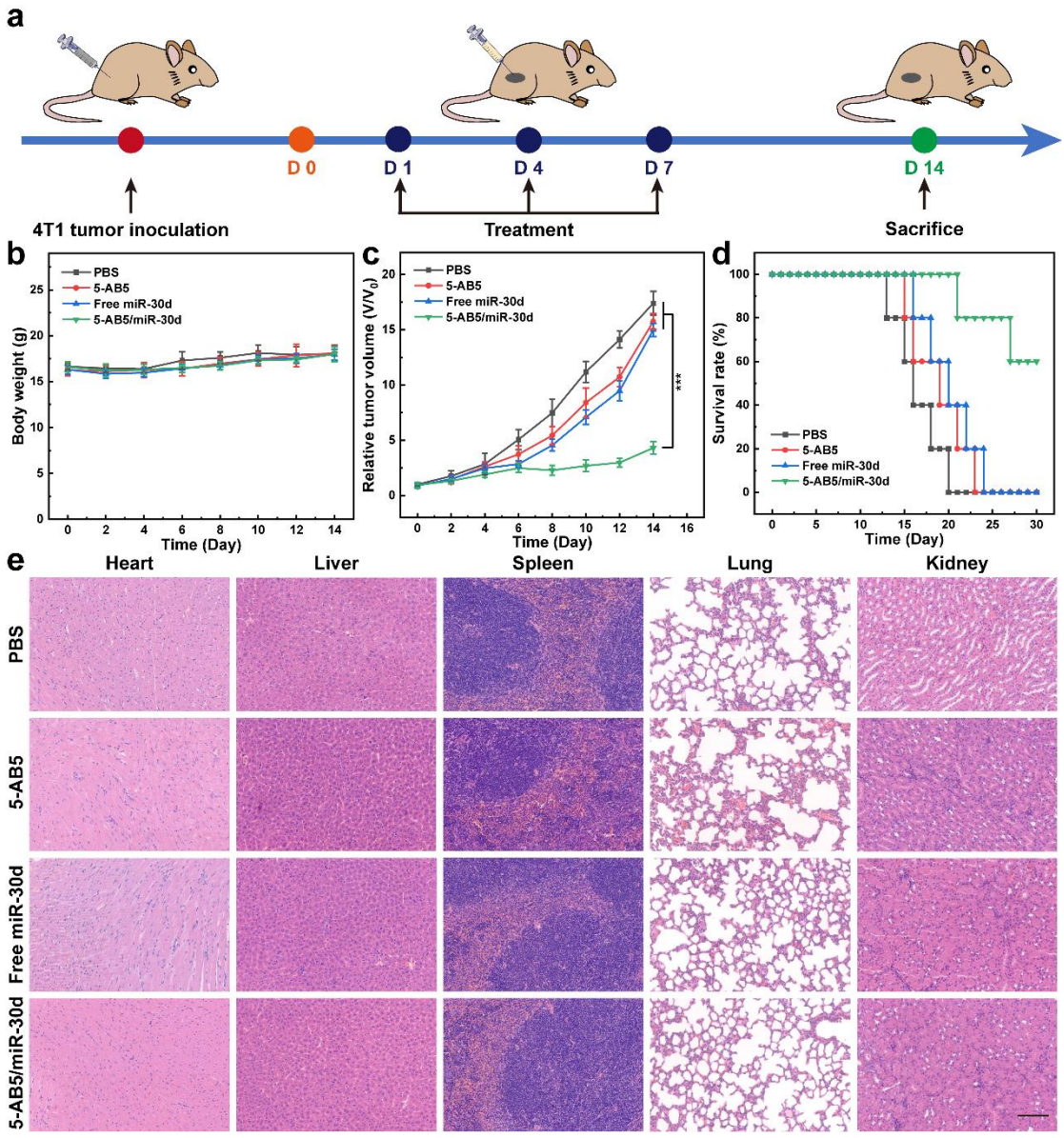

Figure 5. (a) Schematic illustration of tumor treatment schedule. (b) Body weight changes and (c) relative tumor volumes of 4T1 tumor-bearing mice following various treatments (n = 6 for each group). (d) Survival rates of 4T1 tumor-bearing mice after different treatments (n = 5 for each group). (e)

Representative H&E-stained sections of main organs collected from the 4T1 tumor-bearing mice after different treatments for 14 days (scale bar = 100 μm for each panel). For c, *** for $p < 0.001$.

Meanwhile, we checked the biosafety profile of the 5-AB5/miR-30d polyplexes for potential translation applications. The major organs of tumor-bearing mice (heart, liver, spleen, lung, and kidney) in different treatment groups were stained by hematoxylin and eosin (H&E, Figure 5e). Apparently, all main organs of mice in different treatment groups do not have any obvious damage and inflammation infiltration, thus demonstrating the good biocompatibility of the developed 5-AB5/miR-30d polyplexes as well as other control materials, similar to the negative PBS control. Moreover, blood routine and serum biochemistry tests were also performed using blood of healthy mice in different treatment groups (Figure S17 and Figure S18). Compared with the PBS control group, all treatments with different materials do not seem to have any significant impacts in terms of all the tested parameters, suggesting the superior biosafety of the developed dendrimer/miR-30d polyplexes.

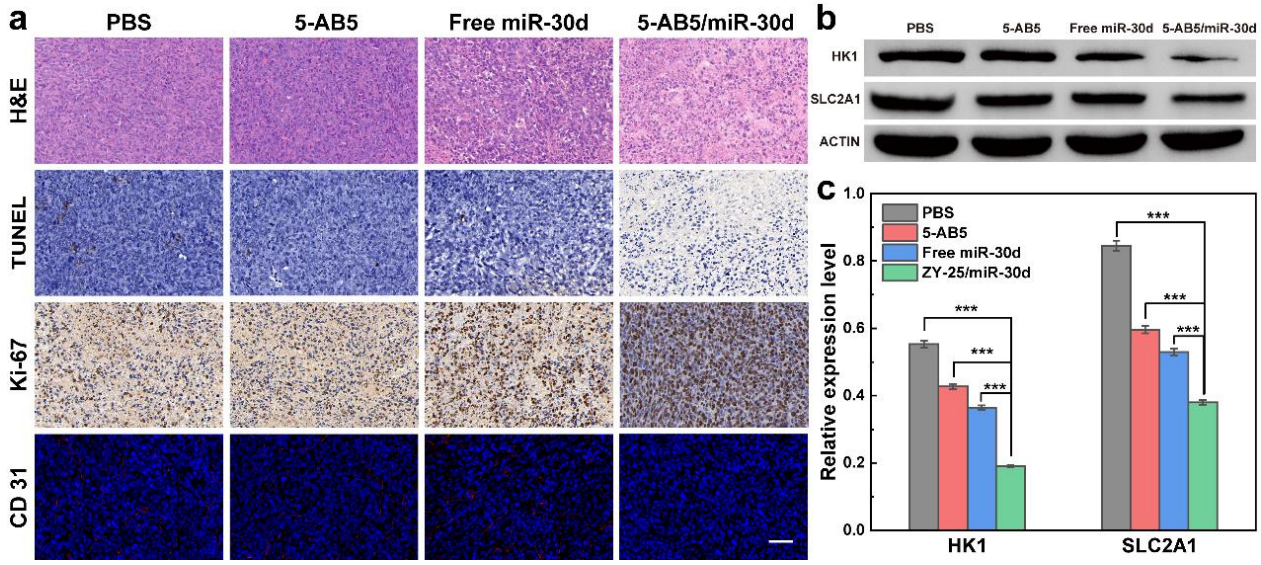

Figure 6. (a) H&E-, TUNEL-, Ki-67- and CD31-stained 4T1 tumor sections on the 14th day after various treatments (Scale bar = 50 μm for each panel). (b) WB analysis of the expression levels of HK1 and SLC2A1 in 4T1 tumors after different treatments. Actin was used as control. (d) Quantitative analysis of HK1 and SLC2A1 protein expressions in 4T1 tumors obtained from the WB assay data *in vivo*. For c, *** for $p < 0.001$.

The tumor therapeutic effect of 5-AB5/miR-30d polyplexes was lastly validated by H&E, TdT-mediated dUTP nick end labeling (TUNEL), and Ki67 stainings (Figure 6a). Clearly, tumors treated with the 5-AB5/miR-30d polyplexes show the largest population of necrotic and apoptotic tumor cells and the best proliferation inhibition efficacy, elaborating the best therapeutic effect of the dendrimer-mediated gene delivery. Next, the tumor slices were immunohistochemically stained to examine the CD31 expression to verify the anti-angiogenesis effect of miR-30d delivery. As shown in Figure 6a, the treatment of 5-AB5/miR-30d polyplexes leads to much less CD31 expression than other groups, further illustrating their enhanced anti-angiogenesis effect of tumor cells *in vivo* through gene therapy. As can be seen in Figure 6b-c, HK1 and SLC2A1 protein expressions in 4T1 tumors are all downregulated in different treatment groups in comparison to the PBS control, and the group of 5-AB5/miR-30d has the most significant downregulation of HK1 and SLC2A1 proteins among all groups ($p < 0.001$). Overall, the created 5-AB5/miR-30d polyplexes could be employed as an effective means for gene therapy of tumors *in vivo*.

4. Conclusion

We have developed unsymmetrical cationic phosphorus dendrimers as a platform to deliver miR-30d for breast cancer therapy. Through a divergent approach, unsymmetrical 5-AB5 dendrimers bearing 5 pyrrolidinium groups and one primary amine group on each dendrimer surface can be synthesized and protonated to be positively charged, thus leading to effective compaction of miR-30d through electrostatic interaction. Under an optimized N/P ratio of 10, the developed 5-AB5/miR-30d polyplexes display the best gene delivery efficiency, allowing for effective cell migration and outstanding inhibition of the HK1 and SLC2A1 protein expressions *in vitro*. The therapeutic efficacy of 5-AB5/miR-30d polyplex-mediated cancer gene therapy have also been proven in an *in-vivo* murine breast cancer model, where the 5-AB5-mediated miR-30d delivery can also lead to significant downregulation of glycolysis-associated SLC2A1 and HK1 expressions. Since the developed

unsymmetrical low-generation cationic phosphorus dendrimers of 5-AB5 display simple composition and backbone structure and can be further modified through the other part of primary amine group, many more opportunities related to the use of unsymmetrical low-generation cationic phosphorus dendrimers for nanomedicine applications should be expected.

Acknowledgements

Financial supports from the National Key Research and Development Program (2022YFE0196900), the National Natural Science Foundation of China (52350710203), the Science and Technology Commission of Shanghai Municipality (23WZ2503300, 23520712500, 21490711500, and 20DZ2254900), and the Shanghai Education Commission through the leading talent program are gratefully acknowledged. Y.Z. thanks the China Scholarship Council for support.

References

1. Dunbar, C. E.; High, K. A.; Joung, J. K.; Kohn, D. B.; Ozawa, K.; Sadelain, M., Gene therapy comes of age. *Science* **2018,** *359* (6372), eaan4672.

2. Fang, H.; Guo, Z.; Chen, J.; Lin, L.; Hu, Y.; Li, Y.; Tian, H.; Chen, X., Combination of epigenetic regulation with gene therapy-mediated immune checkpoint blockade induces anti-tumour effects and immune response in vivo. *Nat. Commun.* **2021,** *12* (1), 6742.

3. Naldini, L., Gene therapy returns to centre stage. *Nature* **2015,** *526* (7573), 351–360.

4. Di Leva, G.; Croce, C. M., miRNA profiling of cancer. *Curr. Opin. Genet. Dev.* **2013,** *23* (1), 3–11.

5. Ganju, A.; Khan, S.; Hafeez, B. B.; Behrman, S. W.; Yallapu, M. M.; Chauhan, S. C.; Jaggi, M., miRNA nanotherapeutics for cancer. *Drug discovery today* **2017,** *22* (2), 424–432.

6. Reddy, K. B., MicroRNA (miRNA) in cancer. *Cancer Cell Int.* **2015,** *15* (1), 1–6.

7. Ye, J.; Xu, M.; Tian, X.; Cai, S.; Zeng, S., Research advances in the detection of miRNA. *J. Pharm. Anal.*

2019, *9* (4), 217–226.

8. Sahin, U.; Karikó, K.; Türeci, Ö., mRNA-based therapeutics — developing a new class of drugs. *Nat. Rev. Drug Discovery* **2014,** *13* (10), 759-780.

9. Fang, H.; Chen, Q., Applications and challenges of biomaterial mediated mRNA delivery. *Explor. Targeted Anti-Tumor Ther.* **2022**, 428-444.

10. Ghafouri-Fard, S.; Shoorei, H.; Taheri, M., miRNA profile in ovarian cancer. *Exp. Mol. Pathol.* **2020,** *113*, 104381.

11. Fehlmann, T.; Kahraman, M.; Ludwig, N.; Backes, C.; Galata, V.; Keller, V.; Geffers, L.; Mercaldo, N.; Hornung, D.; Weis, T., Evaluating the use of circulating microRNA profiles for lung cancer detection in symptomatic patients. *JAMA Oncol.* **2020,** *6* (5), 714–723.

12. Lanzillotti, C.; De Mattei, M.; Mazziotta, C.; Taraballi, F.; Rotondo, J. C.; Tognon, M.; Martini, F., Long non-coding RNAs and microRNAs interplay in osteogenic differentiation of mesenchymal stem cells. *Front. Cell Dev. Biol.* **2021,** *9*, 646032.

13. Xue, X.; Li, J.; Fan, Y.; Shen, M.; Shi, X., Gene silencing-mediated immune checkpoint blockade for tumor therapy boosted by dendrimer-entrapped gold nanoparticles. *Sci. China Mater.* **2021,** *64* (8), 2045-2055.

14. Hayder, M.; Poupot, M.; Baron, M.; Nigon, D.; Turrin, C.-O.; Caminade, A.-M.; Majoral, J.-P.; Eisenberg, R. A.; Fournié, J.-J.; Cantagrel, A., A phosphorus-based dendrimer targets inflammation and osteoclastogenesis in experimental arthritis. *Sci. Transl. Med.* **2011,** *3* (81), 81ra35–81ra35.

15. Annese, T.; Tamma, R.; De Giorgis, M.; Ribatti, D., microRNAs biogenesis, functions and role in tumor angiogenesis. *Front. Oncol.* **2020,** *10*, 581007.

16. Li, J.; Chen, L.; Sun, H.; Zhan, M.; Laurent, R.; Mignani, S.; Majoral, J.-P.; Shen, M.; Shi, X., Cationic phosphorus dendron nanomicelles deliver microRNA mimics and microRNA inhibitors for enhanced anti-inflammatory therapy of acute lung injury. *Biomater. Sci.* **2023,** *11* (4), 1530–1539.

17. Mignani, S.; Shi, X.; Ceña, V.; Majoral, J.-P., Dendrimer–and polymeric nanoparticle–aptamer bioconjugates as nonviral delivery systems: A new approach in medicine. *Drug Discovery Today* **2020,** *25* (6), 1065–1073.

18. Shirjang, S.; Mansoori, B.; Asghari, S.; Duijf, P. H. G.; Mohammadi, A.; Gjerstorff, M.; Baradaran, B., MicroRNAs in cancer cell death pathways: Apoptosis and necroptosis. *Free Radicals Biol. Med.* **2019,** *139*, 1–15.

19. Hou, Y.; Zhang, Q.; Pang, W.; Hou, L.; Liang, Y.; Han, X.; Luo, X.; Wang, P.; Zhang, X.; Li, L.; Meng, X., YTHDC1-mediated augmentation of miR-30d in repressing pancreatic tumorigenesis via attenuation of RUNX1-induced transcriptional activation of Warburg effect. *Cell Death Differ.* **2021,** *28* (11), 3105-3124.

20. Yin, H.; Wang, Y.; Wu, Y.; Zhang, X.; Zhang, X.; Liu, J.; Wang, T.; Fan, J.; Sun, J.; Yang, A.; Zhang, R., EZH2-mediated Epigenetic Silencing of miR-29/miR-30 targets LOXL4 and contributes to Tumorigenesis, Metastasis, and Immune Microenvironment Remodeling in Breast Cancer. *Theranostics* **2020,** *10* (19), 8494-8512.

21. Pardi, N.; Hogan, M. J.; Porter, F. W.; Weissman, D., mRNA vaccines — a new era in vaccinology. *Nat. Rev. Drug Discovery* **2018,** *17* (4), 261-279.

22. Li, J.; Shen, M.; Shi, X., Poly(amidoamine) Dendrimer-Gold Nanohybrids in Cancer Gene Therapy: A Concise Overview. *ACS Appl. Bio Mater.* **2020,** *3* (9), 5590-5605.

23. Proudfoot, N. J.; Furger, A.; Dye, M. J., Integrating mRNA processing with transcription. *Cell* **2002,** *108* (4), 501–512.

24. Chen, L.; Cao, L.; Zhan, M.; Li, J.; Wang, D.; Laurent, R.; Mignani, S.; Caminade, A.-M.; Majoral, J.-P.; Shi, X., Engineered stable bioactive per se amphiphilic phosphorus dendron nanomicelles as a highly efficient drug delivery system to take down breast cancer in vivo. *Biomacromolecules* **2022,** *23* (7), 2827–2837.

25. Shcharbin, D.; Bryszewska, M.; Mignani, S.; Shi, X.; Majoral, J.-P., Phosphorus dendrimers as powerful

nanoplatforms for drug delivery, as fluorescent probes and for liposome interaction studies: A concise overview. *Eur. J. Med. Chem.* **2020,** *208*, 112788.

26. Chen, L.; Li, J.; Fan, Y.; Qiu, J.; Cao, L.; Laurent, R.; Mignani, S.; Caminade, A.-M.; Majoral, J.-P.; Shi, X., Revisiting Cationic Phosphorus Dendrimers as a Nonviral Vector for Optimized Gene Delivery Toward Cancer Therapy Applications. *Biomacromolecules* **2020,** *21* (6), 2502-2511.

27. Chen, L.; Zhan, M.; Li, J.; Cao, L.; Sun, H.; Laurent, R.; Mignani, S.; Caminade, A.-M.; Majoral, J.-P.; Shi, X., Amphiphilic phosphorous dendron micelles co-deliver microRNA inhibitor and doxorubicin for augmented triple negative breast cancer therapy. *J. Mater. Chem. B* **2023,** *11*, 5483-5493.

28. Knauer, N.; Pashkina, E.; Aktanova, A.; Boeva, O.; Arkhipova, V.; Barkovskaya, M.; Meschaninova, M.; Karpus, A.; Majoral, J.-P.; Kozlov, V., Effects of Cationic Dendrimers and Their Complexes with microRNAs on Immunocompetent Cells. *Pharmaceutics* **2022,** *15* (1), 148.

29. Mignani, S.; Tripathi, R. P.; Chen, L.; Caminade, A.-M.; Shi, X.; Majoral, J.-P., New ways to treat tuberculosis using dendrimers as nanocarriers. *Pharmaceutics* **2018,** *10* (3), 105.

30. Mignani, S.; Shi, X.; Rodrigues, J.; Tomas, H.; Karpus, A.; Majoral, J.-P., First-in-class and best-in-class dendrimer nanoplatforms from concept to clinic: Lessons learned moving forward. *Eur. J. Med. Chem.* **2021,** *219*, 113456.

31. Qiu, J.; Chen, L.; Zhan, M.; Laurent, R.; Bignon, J.; Mignani, S.; Shi, X.; Caminade, A.-M.; Majoral, J.-P., Facile synthesis of amphiphilic fluorescent phosphorus dendron-based micelles as antiproliferative agents: first investigations. *Bioconjugate Chem.* **2021,** *32* (2), 339–349.

32. Mignani, S.; Shi, X.; Guidolin, K.; Zheng, G.; Karpus, A.; Majoral, J.-P., Clinical diagonal translation of nanoparticles: Case studies in dendrimer nanomedicine. *J. Controlled Release* **2021,** *337*, 356–370.

33. Wang, D.; Chen, L.; Gao, Y.; Song, C.; Ouyang, Z.; Li, C.; Mignani, S.; Majoral, J.-P.; Shi, X.; Shen, M., Impact of molecular rigidity on the gene delivery efficiency of core-shell tecto dendrimers. *J. Mater. Chem. B*

2021, *9* (31), 6149-6154.

34. Zhan, M.; Wang, D.; Zhao, L.; Chen, L.; Ouyang, Z.; Mignani, S.; Majoral, J.-P.; Zhao, J.; Zhang, G.; Shi, X.; Shen, M., Phosphorus core–shell tecto dendrimers for enhanced tumor imaging: the rigidity of the backbone matters. *Biomater. Sci.* **2023**, DOI:10.1039/d3bm01198d.

35. Xiao, Y.; Wang, M.; Lin, L.; Du, L.; Shen, M.; Shi, X., Integration of aligned polymer nanofibers within a microfluidic chip for efficient capture and rapid release of circulating tumor cells. *Mater. Chem. Front.* **2018,** *2* (5), 891-900.

36. Zhao, Y.; Fan, Z.; Shen, M.; Shi, X., Hyaluronic Acid-Functionalized Electrospun Polyvinyl Alcohol/Polyethyleneimine Nanofibers for Cancer Cell Capture Applications. *Adv. Mater. Interfaces* **2015,** *2* (15), 1500256.

Graphic Abstract